NASA/TM—2019-220328

Static Torsion Testing and Modeling of a Variable Thickness Hybrid Composite Bull Gear

Joel P. Johnston
Universities Space Research Association, Glenn Research Center, Cleveland, Ohio

Albert R. Allen
Langley Research Center, Hampton, Virginia

Kelsen E. LaBerge
U.S. Army Research Laboratory, Glenn Research Center, Cleveland, Ohio

Nathan Jessie
A&P Technology, Inc., Cincinnati, Ohio

Gary D. Roberts
Glenn Research Center, Cleveland, Ohio

December 2019

NASA STI Program . . . in Profile

Since its founding, NASA has been dedicated to the advancement of aeronautics and space science. The NASA Scientific and Technical Information (STI) Program plays a key part in helping NASA maintain this important role.

The NASA STI Program operates under the auspices of the Agency Chief Information Officer. It collects, organizes, provides for archiving, and disseminates NASA's STI. The NASA STI Program provides access to the NASA Technical Report Server—Registered (NTRS Reg) and NASA Technical Report Server—Public (NTRS) thus providing one of the largest collections of aeronautical and space science STI in the world. Results are published in both non-NASA channels and by NASA in the NASA STI Report Series, which includes the following report types:

- TECHNICAL PUBLICATION. Reports of completed research or a major significant phase of research that present the results of NASA programs and include extensive data or theoretical analysis. Includes compilations of significant scientific and technical data and information deemed to be of continuing reference value. NASA counter-part of peer-reviewed formal professional papers, but has less stringent limitations on manuscript length and extent of graphic presentations.

- TECHNICAL MEMORANDUM. Scientific and technical findings that are preliminary or of specialized interest, e.g., "quick-release" reports, working papers, and bibliographies that contain minimal annotation. Does not contain extensive analysis.

- CONTRACTOR REPORT. Scientific and technical findings by NASA-sponsored contractors and grantees.

- CONFERENCE PUBLICATION. Collected papers from scientific and technical conferences, symposia, seminars, or other meetings sponsored or co-sponsored by NASA.

- SPECIAL PUBLICATION. Scientific, technical, or historical information from NASA programs, projects, and missions, often concerned with subjects having substantial public interest.

- TECHNICAL TRANSLATION. English-language translations of foreign scientific and technical material pertinent to NASA's mission.

For more information about the NASA STI program, see the following:

- Access the NASA STI program home page at http://www.sti.nasa.gov

- E-mail your question to help@sti.nasa.gov

- Fax your question to the NASA STI Information Desk at 757-864-6500

- Telephone the NASA STI Information Desk at 757-864-9658

- Write to:
  NASA STI Program
  Mail Stop 148
  NASA Langley Research Center
  Hampton, VA 23681-2199

NASA/TM—2019-220328

Static Torsion Testing and Modeling of a Variable Thickness Hybrid Composite Bull Gear

Joel P. Johnston
Universities Space Research Association, Glenn Research Center, Cleveland, Ohio

Albert R. Allen
Langley Research Center, Hampton, Virginia

Kelsen E. LaBerge
U.S. Army Research Laboratory, Glenn Research Center, Cleveland, Ohio

Nathan Jessie
A&P Technology, Inc., Cincinnati, Ohio

Gary D. Roberts
Glenn Research Center, Cleveland, Ohio

National Aeronautics and
Space Administration

Glenn Research Center
Cleveland, Ohio 44135

December 2019

Acknowledgments

The first author was supported by an appointment to the NASA Postdoctoral Program at the NASA Glenn Research Center, administered by Universities Space Research Association under contract with NASA. The authors would like to acknowledge A&P Technology for their participation in this effort including design and manufacture of the test articles discussed. They would also like to acknowledge the University of Akron for performing the static torsion tests described herein.

This work was sponsored by the Advanced Air Vehicle Program
at the NASA Glenn Research Center

Level of Review: This material has been technically reviewed by technical management.

Available from

NASA STI Program
Mail Stop 148
NASA Langley Research Center
Hampton, VA 23681-2199

National Technical Information Service
5285 Port Royal Road
Springfield, VA 22161
703-605-6000

This report is available in electronic form at http://www.sti.nasa.gov/ and http://ntrs.nasa.gov/

Static Torsion Testing and Modeling of a Variable Thickness Hybrid Composite Bull Gear

Joel P. Johnston
Universities Space Research Association
Glenn Research Center
Cleveland, Ohio 44135

Albert R. Allen
National Aeronautics and Space Administration
Langley Research Center
Hampton, Virginia 23681

Kelsen E. LaBerge
U.S. Army Research Laboratory
Glenn Research Center
Cleveland, Ohio 44135

Nathan Jessie
A&P Technology, Inc.
Cincinnati, Ohio 45245

Gary D. Roberts
National Aeronautics and Space Administration
Glenn Research Center
Cleveland, Ohio 44135

Summary

Torsional strength of a variable thickness hybrid gear web was measured by performing static testing on the part in a large torsion test frame. The outer rim of the hybrid gear web was fixed to the bottom of the test frame and loading was applied to the web through a shaft. The test setup included the installation of digital image correlation (DIC) systems to obtain deformation and strain measurements from the surfaces of the hybrid gear web and the mechanical test equipment to ensure reliability of the test. The results indicated that the variable thickness hybrid gear web achieved approximately twice the torsional strength compared to that of previous hybrid gear designs. The DIC analysis showed significantly more straining of the loading shaft than the actual test article. Additionally, the results demonstrated the importance and affect that the metallic, lobed interlock features had on the principal strain and out-of-plane displacement fields. The analysis revealed that the fixed outer rim was in fact rotating and a rigid-body motion compensation (RBMC) function was computed to determine the actual rotation of the hub and composite web relative to the outer rim. Modeling simulations were performed for the variable thickness hybrid gear web and correlated well with the RBMC rotational deformation seen in the DIC analysis. In addition to benchmarking the load capacity of the hybrid gear web, measuring its strength is useful information to define the parameters needed for dynamic, endurance, and other testing of the part.

Introduction

The civil and military rotorcraft communities are continuously striving to increase power density while reducing maintenance, noise, and cost. Past Government-funded research and technology development efforts have used power density as the most critical performance metric (Refs. 1 and 2). Composite materials have been considered for use in drive system components as a means of reducing the overall weight of the drive system, particularly for large components like drive shafts and housings (Refs. 3 and 4). The use of composites was extended to gearing in a composite-steel "hybrid" gear concept, which replaces steel in the structural portion of a gear with a lightweight carbon fiber composite (Ref. 5). The composite hybridization of spur gears has been implemented and tested in a high temperature, oil-exposed environment, where the constant thickness composite web of the hybrid spur gear interfaced with the metallic components through nonfastener, interlocking features (Refs. 5 to 8). Experiments performed on these hybrid spur gears included static torsion, modal, and dynamic testing in a gear rig. These studies showed that the hybrid spur gears were capable of surviving in harsh conditions and included experiments with starved oil conditions (Ref. 9). Composite materials have also been applied to large, hybrid bull gear designs using constant thickness laminates with lobed geometries to mechanically interact with the metallic components of the hybrid gear (Ref. 8). This study successfully tested a hybrid bull gear under multiple dynamic load states, and showed that the loading did not alter the vibration or thermal performance of the gear. While these tests demonstrated the feasibility of composite integration, the run conditions were limited due to low static torque values measured for this gear design.

In an effort to improve the design, both the composite prepreg layup and the lobed mechanical interlock at the hub were redesigned. The composite web was altered to a variable thickness laminate design in order to improve the weight benefit and load transfer of the gear. Static torsion testing was conducted for the redesigned variable thickness hybrid gear to determine the strength of the part. Digital image correlation (DIC) camera systems were set up with the static tests to observe any local deformation and failure of the composite, and to study the effect of the lobed interlocks. The loading and deformation data was used to create and validate a finite element model of the gear testing.

Torsion Testing Equipment With Digital Image Correlation Systems

The torsion frame used for this study has a 90° rotational range and a maximum torque capacity of 600,000 in·lbf (67,800 N·m), however, the installed load cell and requirements of the test limited the maximum torque to 240,000 in·lbf (27,100 N·m). The frame, shown in Figure 1(a), was custom built to test the composite components with further details of the design and operation provided by Kohlman (Ref. 10). The blue coloring of the image in this figure is a result of the lighting that was used to improve the measurement accuracy of the DIC systems. The outer rim of the web was bolted to a fixed platform, shown in the center of Figure 1(a), and a 0.2 deg/min rotational deformation rate was applied through a shaft driven by a hydraulic rack and pinion torsion actuator. The testing progressed using this rate until a failure of the test article or an exceedance in the torque meter range occurred. In contrast to the triangular polygon used for the dynamic test articles (Ref. 11), a square polygon interface feature was used for all of the static torsion tests to attach the input loading shaft to the hybrid web. One reason for switching to the square polygon feature was its allowance for easier removal of the shaft from the test article. The input loading shaft transitioned from several circular cross sections of larger diameters to the smaller square polygon profile in order to properly install the loading actuator and transducer.

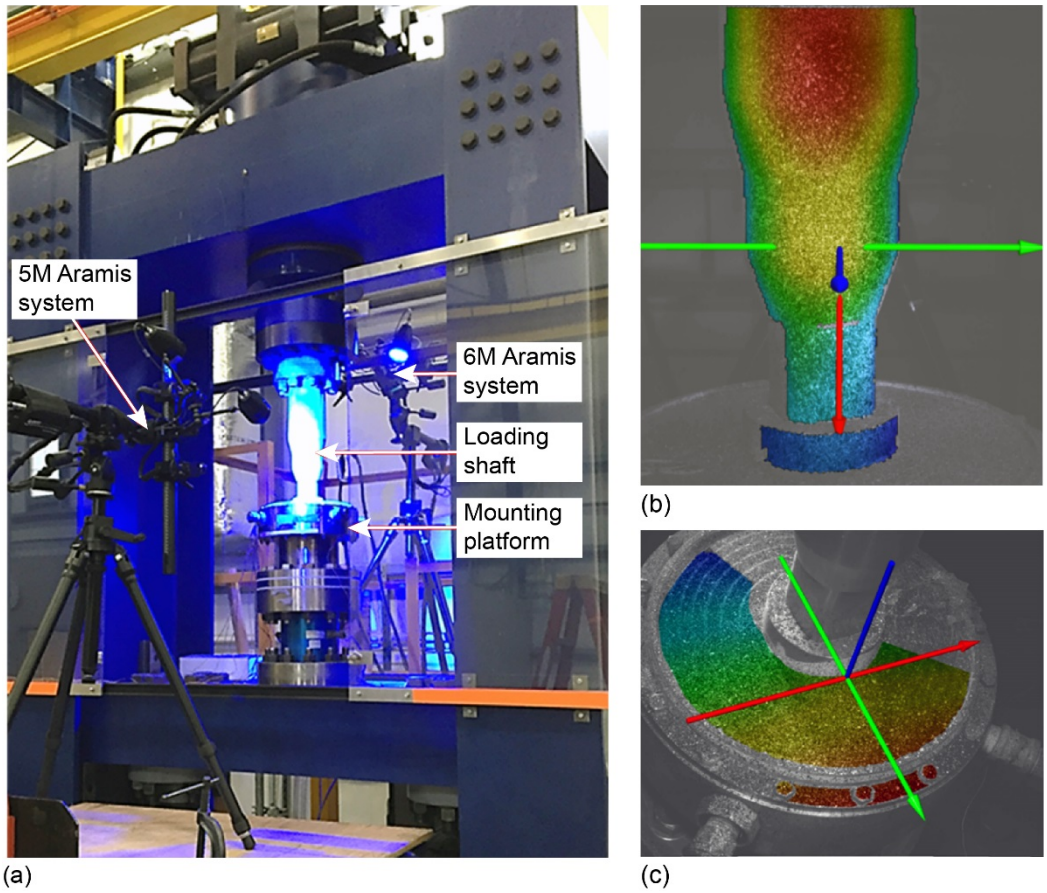

Figure 1.—Static testing setup for the hybrid gear web. (a) Torsion frame with the two GOM ARAMIS systems. (b) Deformation field on input shaft. (c) Deformation field on the hybrid gear web surface.

The DIC measurements were obtained using two ARAMIS systems (GOM) in order to monitor deformation during the test. A 5-megapixel DIC camera system was rotated to fully view the input loading shaft at the front of the test frame. The measurable surface from this DIC system is evident from the displacement contour presented in Figure 1(b). A 6-megapixel DIC camera system was installed at the back of the test frame to observe the surface of the gear web (Figure 1(c)).

Preliminary Hybrid Gear Study

The original, constant thickness hybrid gear web consisted of three main components: an outer steel adapter, an inner steel hub, and composite sections that interfaced with both the inner and outer adapters (Figure 2). Three composite web sections were made with each containing multiple prepreg plies. The lobed mechanical interlocks were cut from the middle composite section to mate with the adjacent metallic adapters. The middle section was captured on either side with the remaining composite sections (referred to as outer capture plies), which constrained the section axially and provided an additional surface for adhesion at the steel-composite interfaces perpendicular to the axis of rotation.

The composite sections were manufactured using a compression molding technique with T700S carbon fiber fabric that was preimpregnated with an epoxy resin (TC–250, Toray Group). The fabric preforms consisted of a quasi-isotropic 0/+60/–60 braid, produced by A&P Technology, with 24,000 tows in the axial direction (0° tows) and 12,000 tows in the bias directions (±60° tows). The inner composite section was made using 16 layers of the braided composite. Each of the layers were rotated to maximize the

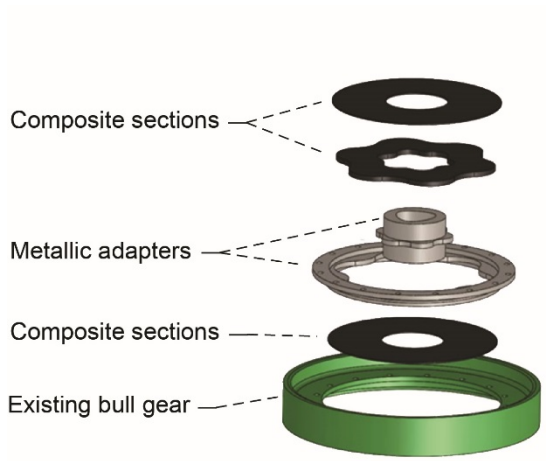

Middle composite section	
Layer	Ply orientation
1	0
2	60
3	–60
4	0
5	60
6	–60
7	0
8	60
9	–60
10	0
11	–60
12	60
13	0
14	–60
15	60
16	0

Outer composite section	
Layer	Ply orientation
1	0
2	60
3	–60
4	–60
5	60
6	0

Figure 2.—Exploded view of the hybrid bull gear with composite sequence definitions.

quasi-isotropic effect of the material as detailed by the laminate sequences in Figure 2. The outer composite sections were made in the same manner as the inner plate, but contained only six layers. The average fiber volume fraction value determined for the composite was approximately 56.4 percent. The steel components were made with a FLEXOR® M steel, produced by the Pennsylvania Steel Corporation, that was prehardened to provide better tolerancing of the part and improve the machining process. A polygon feature was machined into the inner steel hub to interface with the shafting of the gear test rig opposed to a traditional spline feature. The polygon geometry ensured a stronger connection with the shaft and prevented failure of the gear web. The hybrid gear web (Figure 3(a)) was assembled by bonding and pressing all the steel and composite parts together using a bonding jig, which both heated and properly aligned the pieces, and applied a compatible film adhesive (MTA® 241, Solvay) that had the same glass transition temperature as the epoxy resin. A cocured version of the hybrid gear web was also produced by modifying the bonding jig and manufacturing process. One difference in the cocuring process was that the circular geometries and sinusoidal patterns of the lobes were cut into the composite prepreg material before the curing process was applied, as opposed to machining these geometries after curing.

Static torsion tests of various constant thickness hybrid gear webs were conducted to determine the strength of each design and compare the loading responses. One of the secondarily bonded hybrid gears was designed with axial fasteners through the composite and metallic lobes of the mechanical interlock at the inner hub, as presented in Figure 3(b), to prevent through-thickness deformation. The torque plots in Figure 4 show that the cocured and secondarily bonded hybrid webs failed at around 140,000 in·lbf of torque. The torsional strength increased to 180,000 in·lbf for the secondarily bonded hybrid web with the added axial fasteners. The response shows a drop in torque prior to failure at around 100,000 in·lbf for both of the secondarily bonded webs, which was accompanied by an audible noise indicating that minor damage occurred in the part, such as a capture ply debond. Deformation was observed on the pressure side of the axial fasteners due to through-thickness buckling of the material. The plot for the cocured hybrid web also indicates an irregularity in the torque behavior occurring at 100,000 in·lbf, but the gradient of the event was smaller compared to the results of the other hybrid gears. This suggests that there was potentially better adhesion or more surface contact between the composite and metal sections. After the event, the torque redistributed to the internal plies and the web continued to carry load until failure.

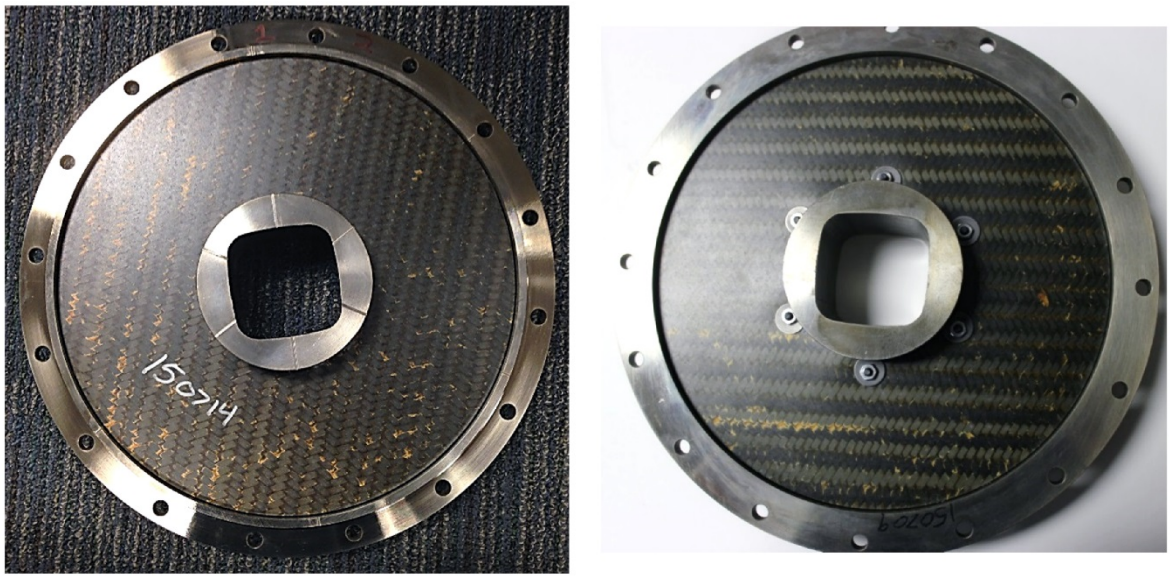

(a) (b)

Figure 3.—Construction of constant thickness hybrid gears. (a) Secondarily bonding the composite sections. (b) Secondarily bonding and applying fasteners through the composite sections.

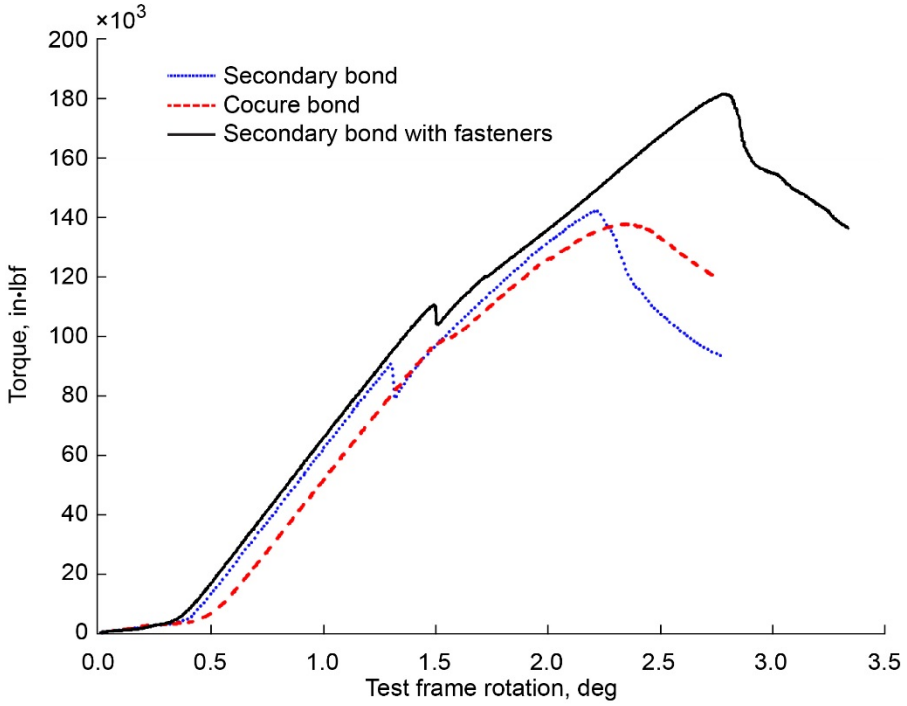

Figure 4.—Torsional responses for constant thickness hybrid gear web tests.

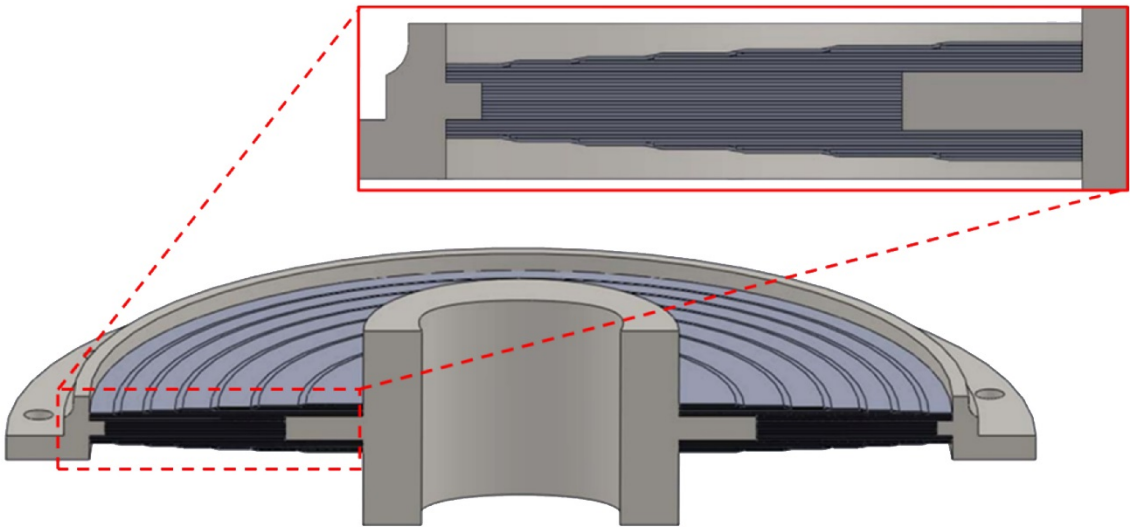

Figure 5.—Cross-sectional view of variable thickness hybrid gear web.

Redesign of Hybrid Gear

The design of the hybrid gear was improved by making small changes to the lobed mechanical interlock geometry at the hub and varying the thickness of the composite web. Given the large torque arm provided by the outer diameter, it was determined the thickness of the gear web could be decreased by as much as 40 percent and the resulting part would still retain the load carrying capability of the previous constant thickness design. Therefore, a series of composite ply drops were integrated into the gear web design to produce a variable thickness gear with fewer plies at the outer diameter. The result was a hybrid gear web with 32 composite layers (0.667 in. thick) at the innermost diameter and 20 composite layers (0.417 in. thick) at the outermost diameter (Figure 5). The preliminary constant thickness web results, discussed in the previous section, demonstrated similar ultimate strength properties between the cocured and secondary bonded gear webs. However, the cocured gear web did not have a sharp drop in load that was present in the secondary bonded gear webs, which was attributed to capture ply debonding. Therefore, the cocuring process was solely utilized to make the redesigned variable thickness hybrid gear and the same constituents were used.

Hybrid Gear Experimental Results

Static torsion experiments were performed on the variable thickness hybrid gear web design using the torsion testing facilities at the University of Akron. The loading response in Figure 6 shows nonlinear behavior in both the torque and axial load for this rotation-controlled test. An initial loading and unloading cycle was performed before this test (not shown) to preload the gear web and ensure it was properly set in the test frame. The load in the axial direction was recorded alongside the torque, but a specific control system was not installed on the frame for the axial load. Therefore, the axial load values shown in the figure are dependent on the deformation and mechanisms associated with the test frame and the hybrid gear. While the axial load values are relatively small compared to the torsional loads, the size of the hybrid gear and location of the axial loading creates a twisting moment that affects the deformation. The gear web endured a torsional load of 240,000 in·lbf (27,100 N·m), the maximum allowed by the apparatus, without experiencing a failure.

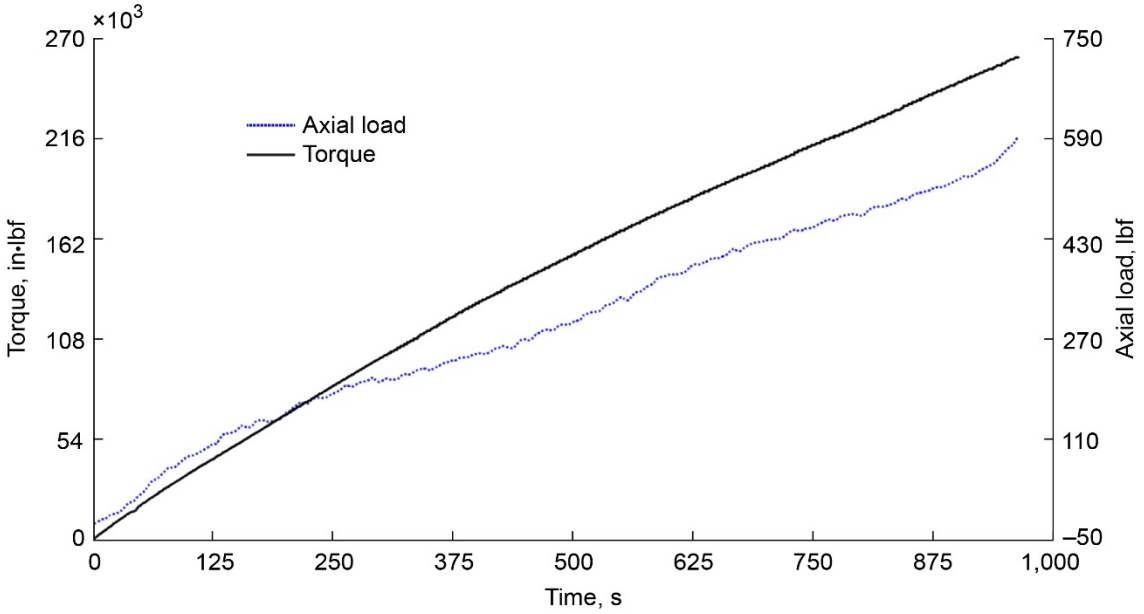

Figure 6.—Loading response during the test.

Data from the DIC systems was analyzed to determine if there was any noticeable deformation or failure of the hybrid gear web, specifically near the interlocks. In order to quantitatively measure the deformation and effect of the interlocks, the DIC data was averaged from several measurement areas of specific features from the loading shaft and hybrid web as indicated in Figure 7. An image of the hybrid gear web model is used as the background of Figure 7(a) to illustrate the placement of the DIC measurement areas with respect to the lobed interlock structure, which can be seen for both the outer rim and the inner hub. In this image, the outer composite layers are hidden in order to view the inner composite layers and lobed interlock structure of the gear web (darker crosshatched area). The transparent gray area overlaid on the model is the complete observable surface computed by the DIC system and software. The irregularity and holes in the right portion of this surface are due to wiring for the test setup. The seven ply drops, which produce the tapered geometry of the hybrid gear web, are also evident in the surface composite layer of the figure. The ply drops create plateaus (also called “steps”) on the composite surface, and an areal DIC measurement was obtained from each of these steps. However, the viewing angle of the DIC system prevented measurements from the step closest to the outer rim. Therefore, only measurements from six of the steps are shown in the subsequent plots. The red areas in the figure depict the measurements taken from areas between the inner lobe structure and the blue areas represent the measurement set extracted from the surface over the inner lobe structure (denoted as “at lobe” in subsequent plots in this report), approximately 30° from the first set. Principal strain results are presented in Figure 8 for areas on the hybrid gear web using both sets of measurement areas. The plots exhibit the straining of the web during the loading phase, which ends at 965 s, as well as a small portion of the unloading phase. Comparison of these results demonstrates a significant difference between the two sets of DIC areas, where Step 1 of the composite experienced approximately 40 percent more strain between the lobes than the area over the lobes. This strain gradient decreased in the steps closer to the outer rim of the composite, with the strain at Steps 5 and 6 of the composite showing little difference between the two sets of measurements. While these strain comparisons establish the effect of the gear web architecture, it is important to note that the straining of the gear web was minimal where the maximum value was smaller than 0.25 percent, which further verifies the load carrying capability of the variable thickness hybrid gear design.

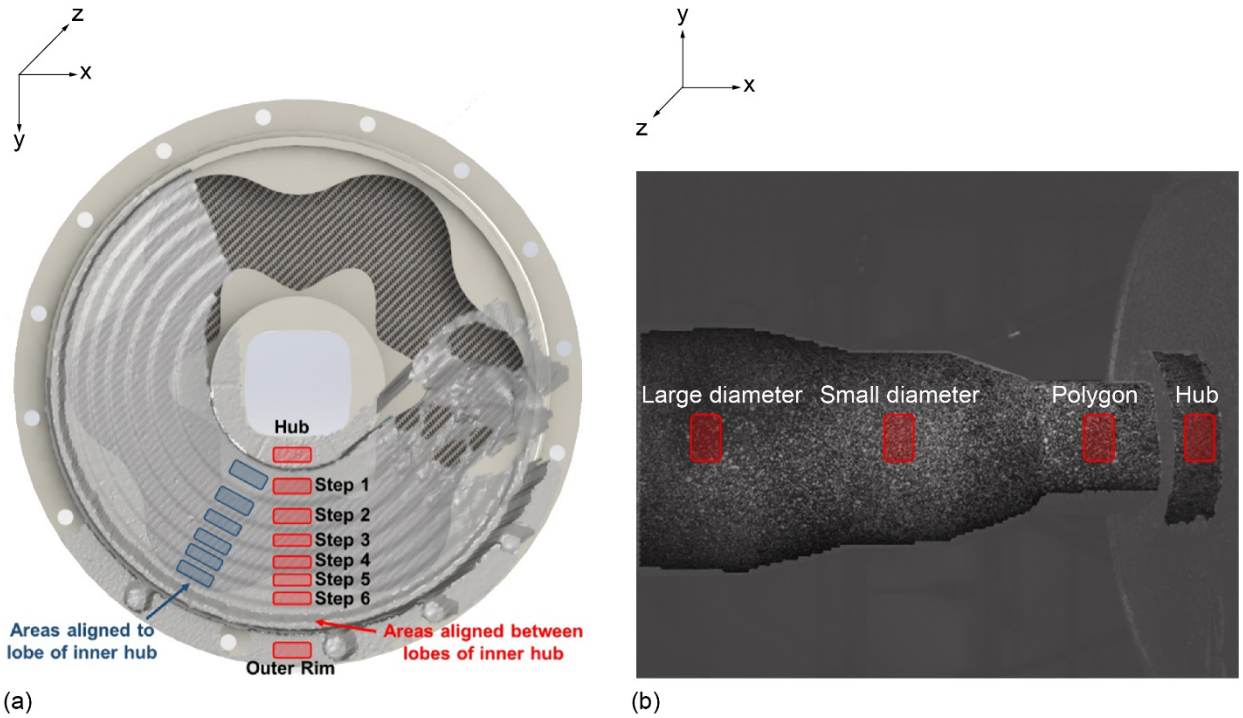

Figure 7.—Measurement areas from the digital image correlation (DIC) systems. (a) Hybrid web. (b) Loading shaft of the test frame.

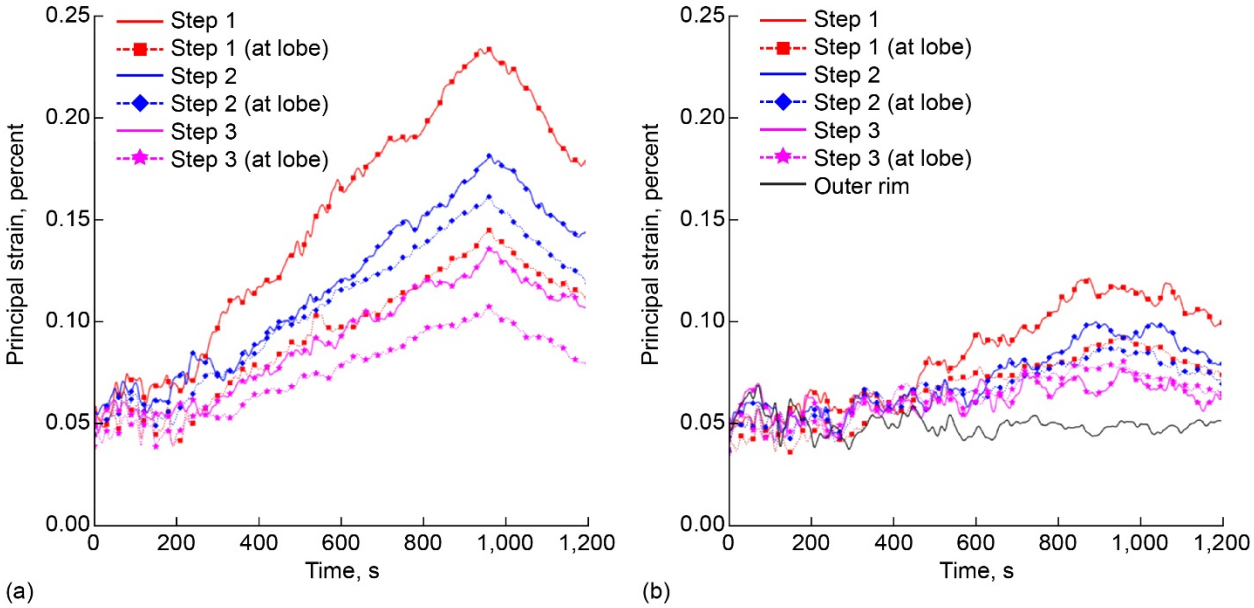

Figure 8.—Average principal strain measurements. (a) Steps 1 to 3. (b) Steps 4 to 6 and the outer rim.

The average rotation was computed from the areal data to observe the effect of the lobed mechanical interlocks and the bolted connections. The measurement areas extracted from the DIC surface of the shaft are shown in Figure 7(b) and each area is aligned with the axis of the shaft. The rotation response of the different areas of the loading shaft is shown in Figure 9(a) where the rotation was largest at the actuator, out of view from the DIC systems, and the gradient drastically decreased at the hub. This large rotation gradient and the small dimensional profile of the polygon section caused large strains to develop near this section of the shaft as shown by the plot in Figure 9(b) and the principal strain contours in Figure 10. Additionally, the strain buildup and rotation of the polygon section causes large strain near the bottom of the hub surface where the hub is the thinnest and where the corner of the polygon section transfers a large amount of stress. The plot demonstrates that the principal strain in the polygon section of the shaft was approximately 50 percent larger than the strain in the web. In contrast, the strain in the large diameter section of the shaft and in Step 6 of the web was minimal in comparison and did not change during the loading or unloading phase of the test.

The rotation plots for each areal measurement on the hybrid gear web are plotted as a function of time in Figure 11. The plots show that a small difference in rotation occurred within the measurements between the inner lobe structure and the measurements on top of the inner metallic lobe. Additionally, this difference in rotation was prominent for several of the steps closest to the inner hub and decreased at steps near the outer rim. The overall rotation response of the web shows several jumps in data with a particularly large spike around 650 s. This spike was evident in both the metallic and composite components viewable by the DIC system, which suggests that this behavior was due to an anomaly in either the mechanical equipment or the measurement system. While the outer rim of gear web was fixed to the base of the mechanical equipment, the results show that rotation occurred in the outer rim and the bolt areas. There are several possible causes for the rotation at the fixed end including shearing of the bolts, damage to the bolt threads, sliding of undersized bolts, and compliance in the fixture for the outer rim.

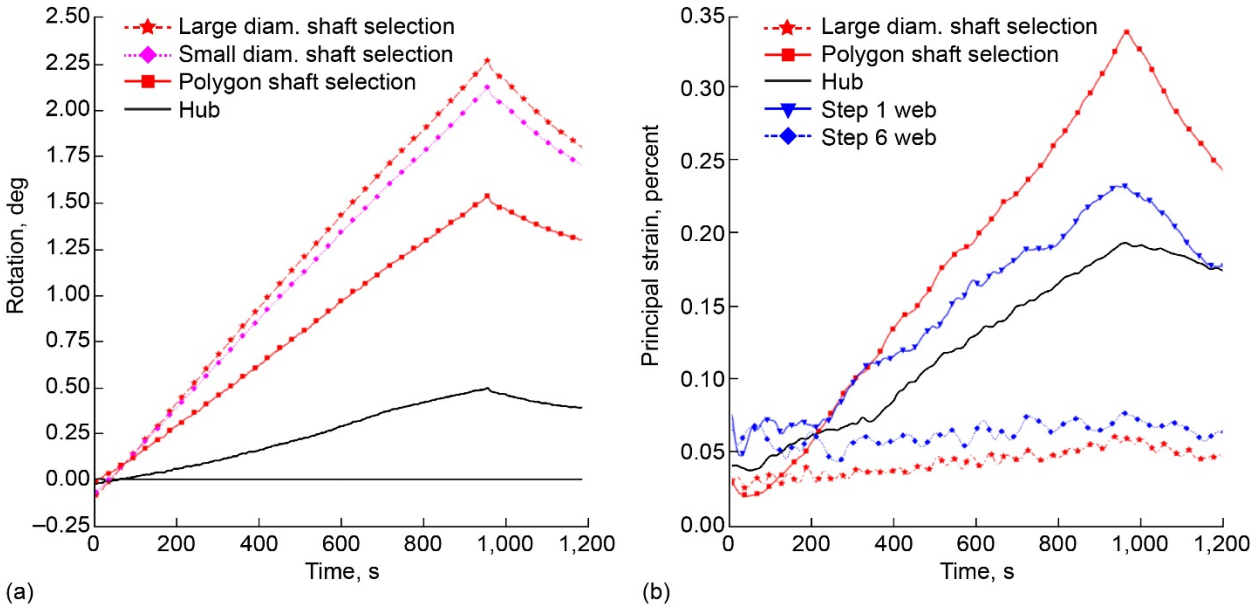

Figure 9.—Digital image correlation (DIC) data plots. (a) Rotation in the loading shaft. (b) Straining of the shaft compared to the gear web.

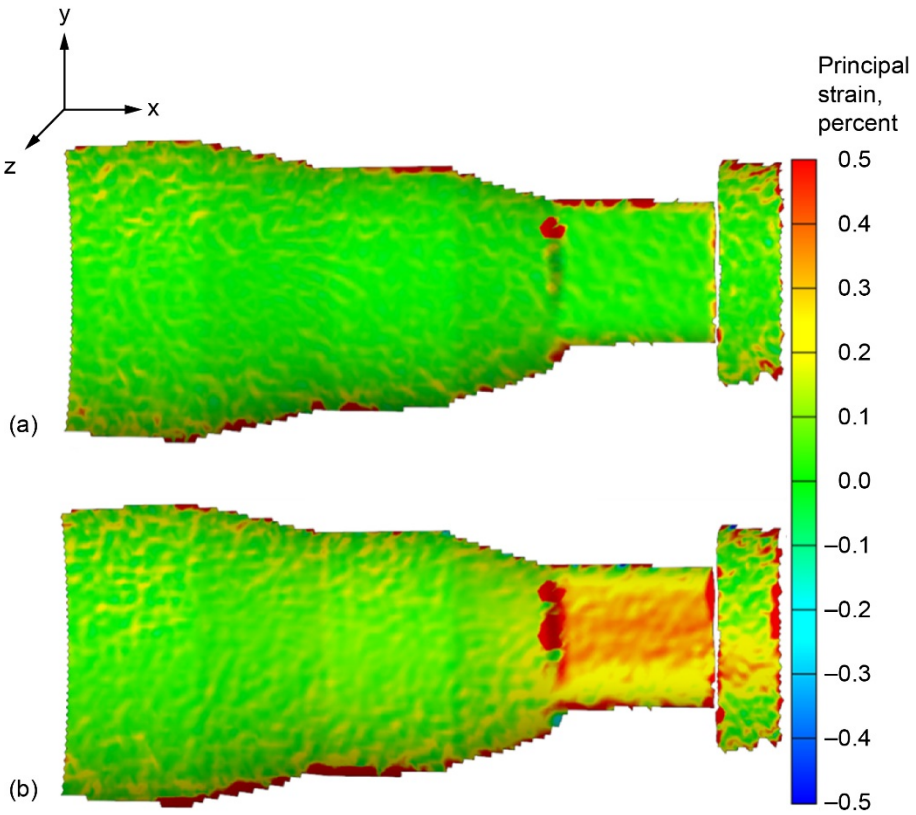

Figure 10.—Principal strain contours of the shaft at different timeframes during the test. (a) 0 s. (b) End of loading at 956 s.

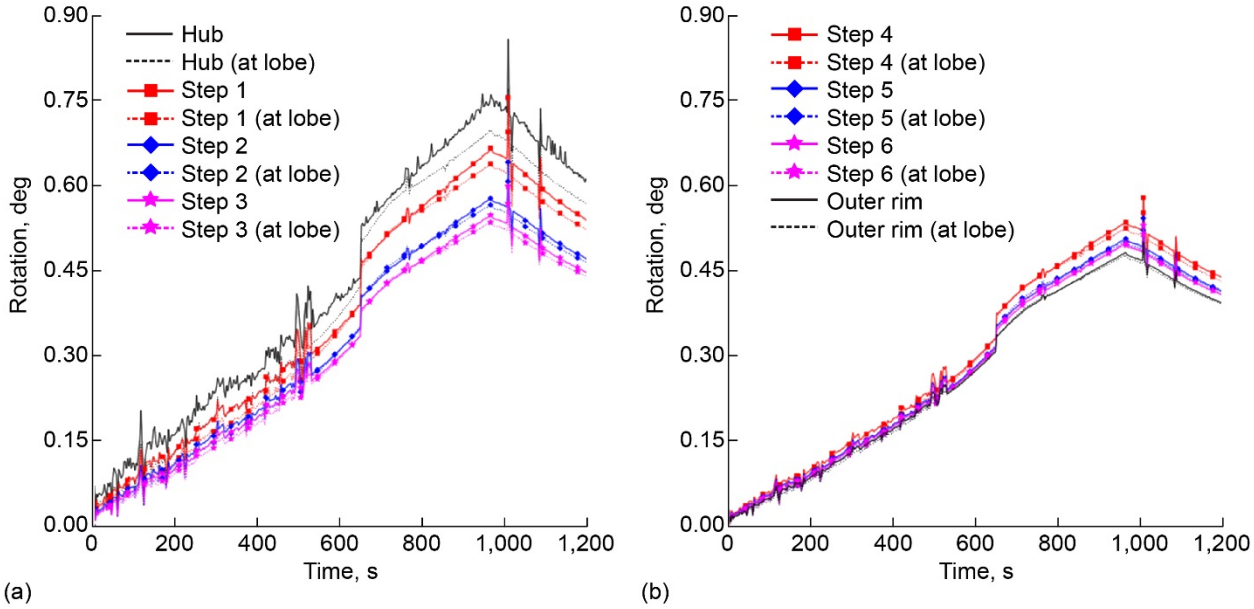

Figure 11.—Average rotation plots of the hybrid web. (a) Hub and Steps 1 to 3. (b) Steps 4 to 6 and the outer rim.

In order to further explain the irregularities in the data, rigid-body motion compensation (RBMC) was applied to the full field data of the hybrid gear web. The compensation was performed, using the RBMC function within the GOM ARAMIS DIC software, by selecting the observable area of the outer rim as a basis for the function. The designation of the outer rim as the function basis makes the assumption that the outer rim is fixed and calculates the deformation of the hybrid gear web relative to the outer rim. Therefore, the compensated rotation plots in Figure 12 exhibit smaller values, compared to the plots in Figure 11, with the smallest rotation value in the outer rim. The rotation plots in Figure 13 focus on the outer rim response and compare it to the rotation of several boltheads. This comparison shows spikes in bolthead rotation occurring in the 600 to 650 s range, which corresponds to the rotation spikes of the

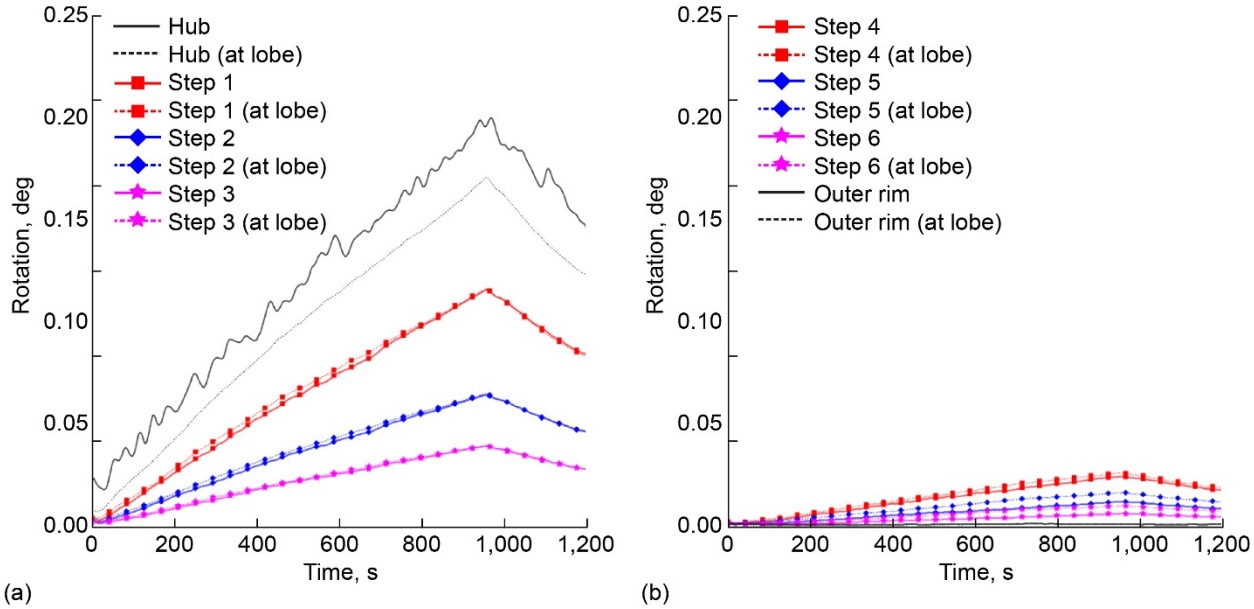

Figure 12.—Hybrid web rotation plots with a rigid-body motion compensation (RBMC) function applied. (a) Hub and Steps 1 to 3. (b) Steps 4 to 6 and the outer rim.

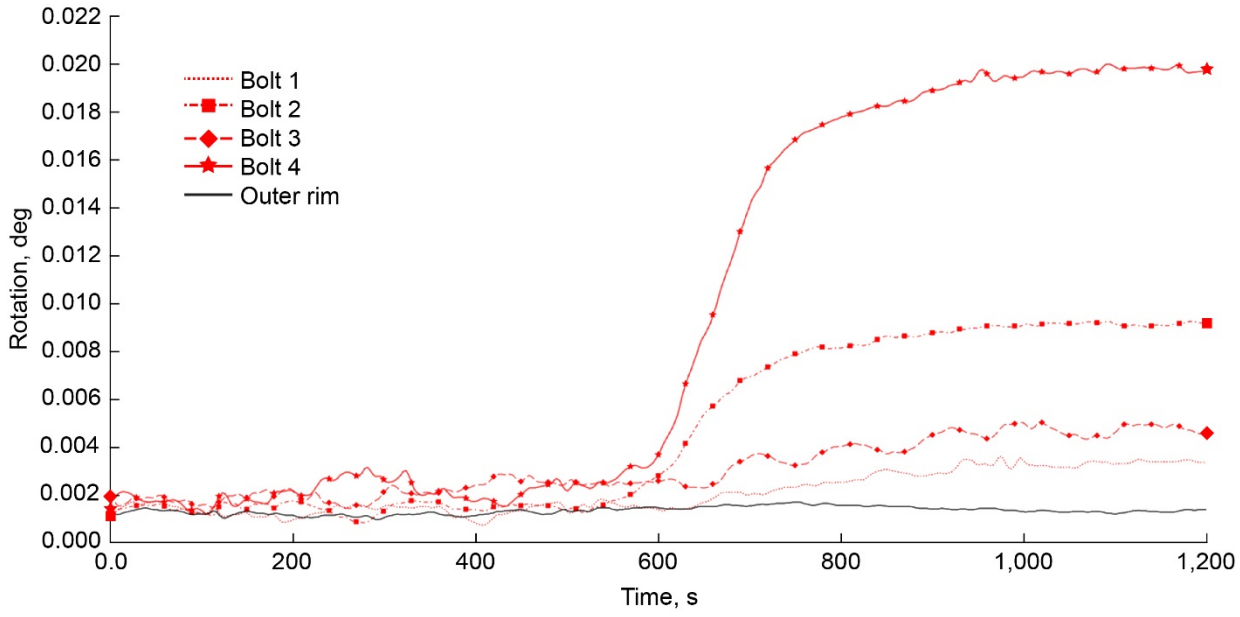

Figure 13.—Rotation of the bolts compared to the outer rim.

uncompensated data (Figure 11). Since the outer rim is effectively fixed through the applied RBMC function, these spikes in bolthead rotation further emphasize the previously stated conjectures suggesting that the bolts are sliding, shearing through the outer rim, or being damaged during the test. A time series of out-of-plane displacement contours, with the RBMC function applied, is presented in Figure 14 and provides a clearer definition of the deformation. The resultant and out-of-plane displacement contours from the final time stage of the test are overlaid on a model of the gear web in Figure 15. The contours from both Figure 14 and Figure 15 highlight the lobed interlock in the hybrid gear, and larger displacements are evident particularly near the two bottom lobes of the polygon hub. The lobed interlock structure around the hub is more pronounced in the out-of-plane contour due to the axial load applied to the hybrid gear web. Additionally, a sinusoidal pattern is evident in the out-of-plane displacement field for the lobed interlock of the outer rim indicating the constraining effect the outer rim lobed interlock had on the hybrid gear web.

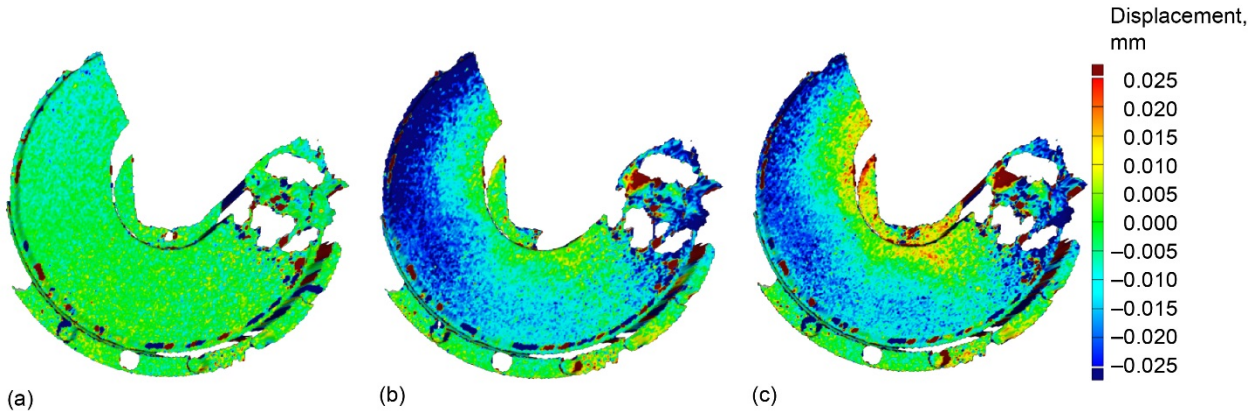

Figure 14.—Out-of-plane displacement contours with rigid-body motion compensation (RBMC) from various time stages. (a) 15 s. (b) 768 s. (c) 951 s.

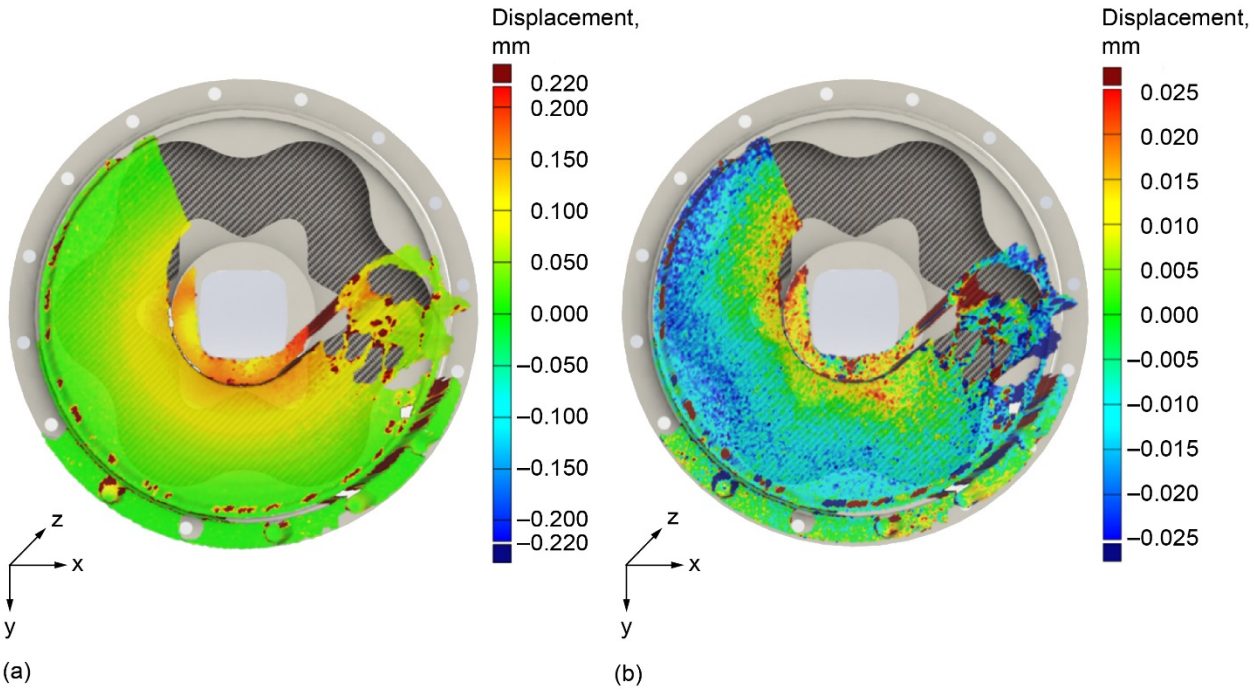

Figure 15.—Displacement contours from the rigid-body motion compensation (RMBC) data overlaid on a model of the hybrid gear. (a) Resultant displacement. (b) Out-of-plane displacement.

Modeling of Hybrid Gear Web

Simulation of the static and dynamic load response of the hybrid gear web and similar transmission system concepts can provide a better understanding of their structural response under a variety of load cases, and may facilitate further concept development while avoiding costly fabrication and testing for each design iteration. Therefore, a finite element model of the variable thickness hybrid gear web was developed and exercised within the Dassault Systèmes' SIMULIA Abaqus computer-aided engineering (CAE) software (Figure 16) to simulate the previously described static torsion test conducted at the University of Akron. Simulation results were then compared with test data in order to validate the modeling approach.

The outer rim and inner hub metallic regions were assigned isotropic properties representative of Pennsylvania Steel Corporation's FLEXOR® M prehardened steel (Ref. 12). The composite region was assigned engineering constants with slight anisotropy based on previous static load and modal tests (Ref. 13). Properties used in the model are summarized in Table I. The finite element model was meshed using 186,339 linear tetrahedral C3D4 elements. Boundary conditions supplied by the torsion test rig were approximated by fixing the interior surfaces of the boltholes on the outer rim bolt and enforcing the torque and axial loads from Figure 6 along the inside surface of the inner hub. Simplifications were made by neglecting axial compression loads along the outer rim boltholes and transferring the torque and axial loads uniformly along the hub's inner surface. The gear rotation shown in Figure 17 was determined by averaging the nodal rotations along the top surface of the inner hub. The simulated gear rotation is plotted in Figure 17(a) alongside the uncompensated test data. The significantly larger rotation of the test data relative to the simulation further suggested that the boundary conditions in the test rig were not rigid. On the contrary, the test data with the applied RBMC function compares favorably with the simulation (Figure 17(b)).

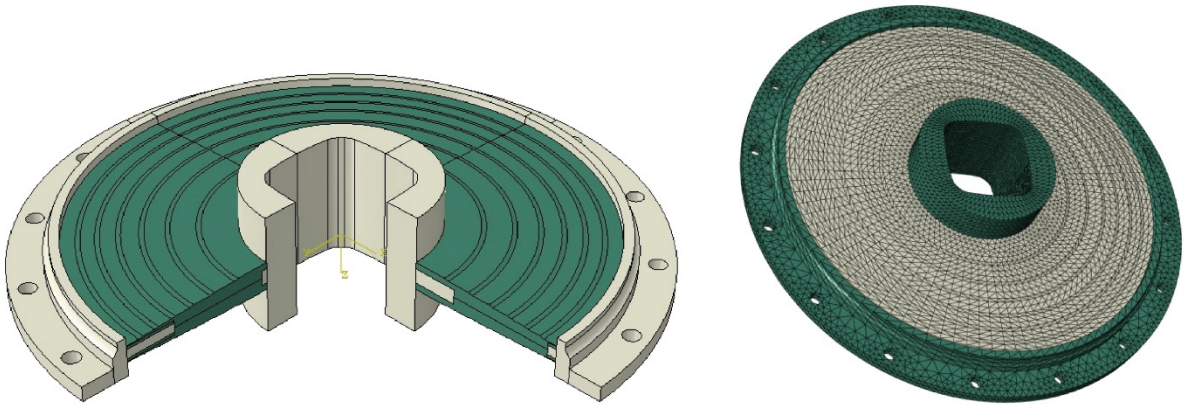

Figure 16.—Variable thickness hybrid gear web. (a) Cutaway view of the tapered thickness gear geometry. Steel components shown in white. Composite laminates shown in green. (b) Corresponding finite element model.

TABLE I.—MATERIAL PROPERTIES USED IN HYBRID WEB MODEL[a]

Steel regions		Composite	
E	30.900	E_1	6.82
ν	0.282	E_2	6.38
---	--------	ν_{12}	0.08
---	--------	G_{12}	464.00

[a]E = Msi. G = ksi. Steel regions = FLEXOR® M (Pennsylvania Steel Corp.). Composite = T700/TC–250 (Toray Group).

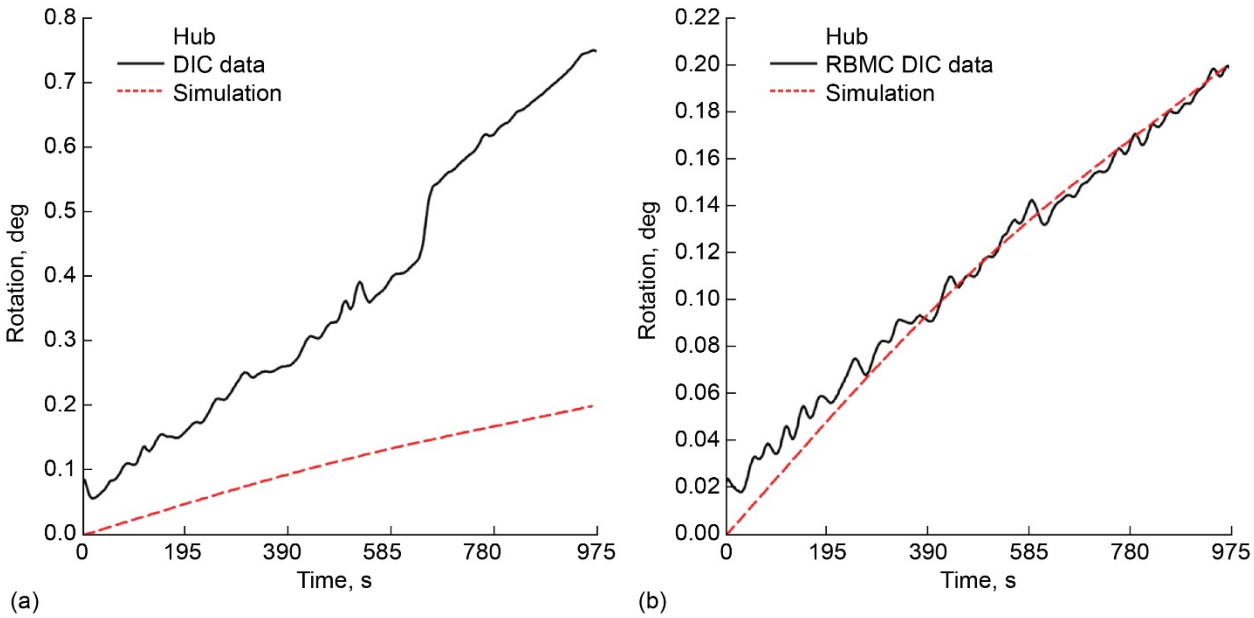

Figure 17.—Comparison of simulated hub rotation results. (a) Uncompensated digital image correlation (DIC) data. (b) DIC data with rigid-body motion compensation (RBMC).

Concluding Remarks

The results from the static torsion testing of the variable thickness hybrid gear web have shown the structural capacity of this part, including the stabilizing effect of the lobed interlocks. The principal strain generated on the loading shaft was larger than the actual test article, which demonstrated the rigidity of the variable thickness hybrid gear web and the inherent difficulty in transferring a large torque through a small profile shaft for any type of mechanical test equipment configuration. The gear web deformation results measured by the digital image correlation (DIC) established that the lobed interlock feature had minimal effect on the rotation for specific locations of the web, but it had a significant effect on the principal strain field. Additionally, measurements from the DIC system showed unexpected rotation in the outer rim of the hybrid gear, which was further explained by applying a rigid-body motion compensation (RBMC) function to the data in the GOM ARAMIS software. The compensated data indicated that complex interactions at the interface between the bolt and outer rim affected the response of the hybrid gear web. A finite element model was constructed for the variable thickness hybrid gear web and the static simulation results correlated well with the compensated DIC rotation data. This redesigned variable thickness hybrid gear web was shown to have at least twice the strength capacity of the previous constant thickness web designs. The improved strength capacity and results from the static testing can be used to define guidelines and specifications for planned durability testing of the variable thickness hybrid web design.

References

1. Anderson, N.E., et al.: Advanced Gearbox Technology Final Report. NASA CR–179625, 1987. http://ntrs.nasa.gov
2. Henry, Zachary S.: Bell Helicopter Advanced Rotorcraft Transmission (ART) Program. NASA CR–195479 (ARL–CF–238), 1995. http://ntrs.nasa.gov

3. Lin, Sherman; and Poster, Scott: Development of a Braided Composite Drive Shaft With Captured End Fittings. Proceedings of the 60th American Helicopter Society International Annual Forum 2004, Baltimore, MD, 2004, pp. 673–687.
4. Cecil, T.; Ehinger, R.; and Kilmain, C.: Application and Configuration Issues of Resin Transfer Molded Composite Transmission Housings—A Program Review. Proceedings of the 63rd American Helicopter Society International Annual Forum 2007, Virginia Beach, VA, 2007, pp. 1327–1335.
5. Handschuh, Robert F.; and Roberts, Gary D.: Hybrid Gear. U.S. Patent 9,296,157 B1, Mar. 2016.
6. Handschuh, Robert F., et al.: Hybrid Gear Preliminary Results—Application of Composites to Dynamic Mechanical Components. NASA/TM—2012-217630, 2012. http://ntrs.nasa.gov
7. Handschuh, Robert F., et al.: Vibration and Operational Characteristics of a Composite-Steel (Hybrid) Gear. NASA/TM—2014-216646 (ARL–TR–6973), 2014. http://ntrs.nasa.gov
8. LaBerge, Kelsen E., et al.: Performance Investigation of a Full-Scale Hybrid Composite Bull Gear. Presented at the American Helicopter Society 72nd Annual Forum, West Palm Beach, FL, 2016.
9. LaBerge, Kelsen E., et al.: Hybrid Gear Performance Under Loss-of-Lubrication Conditions. Proceedings of the 73rd Annual American Helicopter Society International Forum and Technology Display, Fort Worth, TX, 2017, pp. 2250–2256.
10. Kohlman, Lee W.: Evaluation of Test Methods for Triaxial Braid Composites and the Development of a Large Multiaxial Test Frame for Validation Using Braided Tube Specimens. Ph.D. Dissertation, The University of Akron, 2012.
11. LaBerge, Kelsen E., et al.: Evaluation of a Variable Thickness Hybrid Composite Bull Gear. Presented at the American Helicopter Society International 74th Annual Forum & Technology Display, Phoenix, AZ, 2018.
12. FLEXOR® Steel Chemical & Physical Properties. Pennsylvania Steel Corporation, 2016. www.pennsylvaniasteel.com/chemistry-properties.php Accessed Oct. 15, 2019.
13. Littell, Justin D.: Experimental and Analytical Characterization of the Macromechanical Response for Triaxial Braided Composite Materials. NASA/CR—2013-215450, 2013. http://ntrs.nasa.gov